Jun Cai*, Kuaishe Wang, Jiamin Shi, Wen Wang and Yingying Liu

A Modified Double Multiple Nonlinear Regression Constitutive Equation for Modeling and Prediction of High Temperature Flow Behavior of BFe10-1-2 Alloy

DOI 10.1515/htmp-2016-0123
Received June 22, 2016; accepted December 9, 2016

Abstract: Constitutive analysis for hot working of BFe10-1-2 alloy was carried out by using experimental stress–strain data from isothermal hot compression tests, in a wide range of temperature of 1,023~1,273 K, and strain rate range of 0.001~10 s^{-1}. A constitutive equation based on modified double multiple nonlinear regression was proposed considering the independent effects of strain, strain rate, temperature and their interrelation. The predicted flow stress data calculated from the developed equation was compared with the experimental data. Correlation coefficient (R), average absolute relative error ($AARE$) and relative errors were introduced to verify the validity of the developed constitutive equation. Subsequently, a comparative study was made on the capability of strain-compensated Arrhenius-type constitutive model. The results showed that the developed constitutive equation based on modified double multiple nonlinear regression could predict flow stress of BFe10-1-2 alloy with good correlation and generalization.

Keywords: BFe10-1-2 alloy, high temperature flow behavior, modified double multiple nonlinear regression, constitutive equation

Introduction

BFe10-1-2 alloy is a representative of the Cu-Ni alloys which have diverse combinations of corrosion resistance and anti-fouling properties [1, 2]. Therefore, this alloy has a wide range of applications in sea water desalination, shipping and the power industries. The main processing methods of BFe10-1-2 alloy consist of semi-solid ingot casting and followed hot extrusion. Therefore, high temperature deformation is an essential processing step for the microstructure and the mechanical properties of the products [3]. Many defects, such as surface crack (Figure 1(a)), overload (Figure 1(b)) and die fracture (Figure 1(c)), are usually found during the hot extrusion process of cupronickel alloy pipes, which results in considerable problems, such as long process times, high energy consumption, low product yield and high cost. Accordingly, a thorough study of high temperature flow behavior of this material is requisite to properly design the deformation parameters.

Constitutive equations, derived on the basis of empirical, semi-empirical, phenomenological, and physically-based models, are frequently used to describe the flow stress varying with deformation parameters [4]. Among these empirical and semi-empirical models, the Johnson-Cook (JC) model and the Zerilli-Armstrong (ZA) model are currently a part of commercial Finite Element Method (FEM) software. JC model has been widely employed due to the fact that it requires less number of experimental data for evaluation of the material constants and can been used for various materials in a wide range of deformation temperatures and strain rates [5]. ZA model considers coupled strain and temperature effects and has been used to analyze different face-centered cubic (FCC) and body-centered cubic (BCC) materials over different strain rates at temperatures between room temperature and $0.6T_m$ (T_m is the melting point) [6]. Among the phenomenological models, the Arrhenius-type equation has been successfully used to describe the high temperature flow behavior of many metal materials, such as Al-Mn system alloy [7], Ti alloy [8] and aluminum matrix composites [9]. Constitutive equation can represent the flow behavior of metal materials, and is used as input to the FEM code for simulating the response of materials under the specified deformation conditions. The reliability of simulation results is seriously influenced by the accuracy of the constitutive equation. On the basis of the orthogonal experiment and variance analysis, Xiao [10] proposed a constitutive model to describe the elevated temperature flow behavior of TiNiNb alloy. However, this constitutive model ignores the combined effect of influence

***Corresponding author: Jun Cai,** School of Metallurgical Engineering, Xi'an University of Architecture and Technology, Xi'an 710055, China, E-mail: jeffreycai0116@gmail.com
Kuaishe Wang, Jiamin Shi, Wen Wang, Yingying Liu, School of Metallurgical Engineering, Xi'an University of Architecture and Technology, Xi'an 710055, China

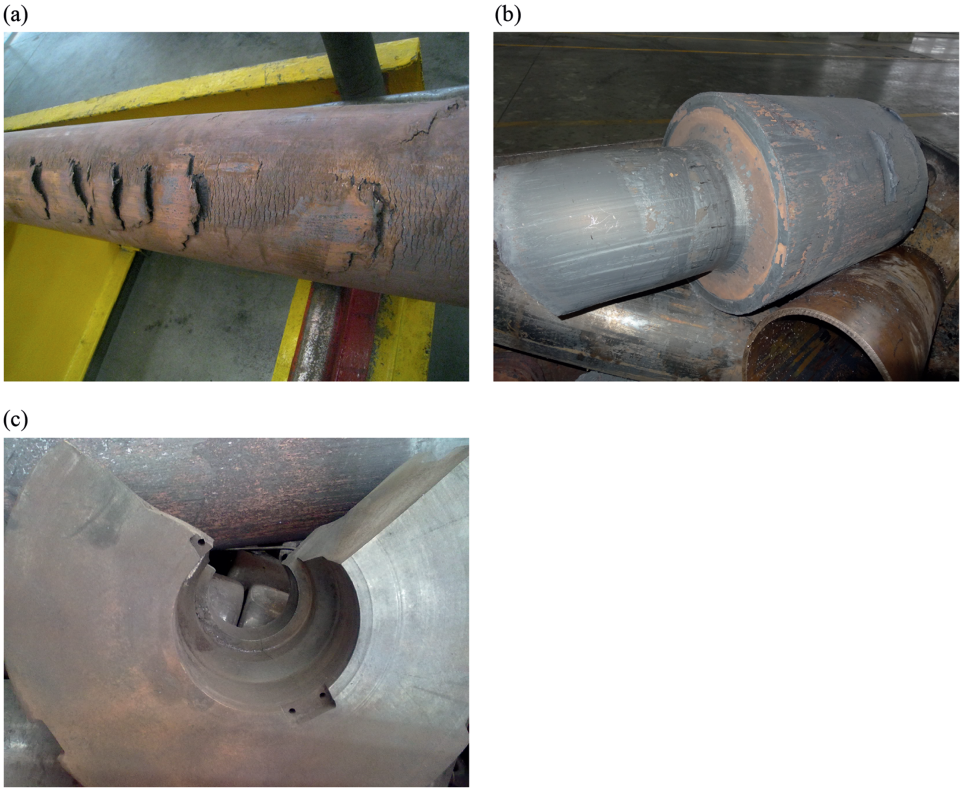

Figure 1: Defect of BFe10-1-2 alloy pipes during hot extrusion (a) surface crack; (b) overload; (c) die fracture.

factors on flow stress, which decreases the accuracy of the constitutive equation. Then, a double multiple nonlinear regression (DMNR) method with higher accuracy is proposed by Yuan [11] to predict the flow behavior of Ti-6Al-4V alloy. However, six analysis factors in DMNR model may not enough, and the major and the inessential analysis factors are not differentiated. Therefore, the main objective of this investigation is to find out a suitable constitutive equation to describe the high temperature flow behavior of BFe10-1-2 alloy with considering the combined effect of strain, strain rate and temperature over a wide range. To achieve our objective, isothermal hot compression tests were performed in the temperature range of 1,023~1,273 K and strain rate range of 0.001~10 s^{-1}. The experimental stress–strain data were then employed to derive a modified double multiple nonlinear regression constitutive equation, which was an amalgam of effect of independent and combined variables. Then, the validity of the developed constitutive equation was examined over the entire range of temperatures and strain rates. Finally, the accuracy of the developed constitutive equation based on modified double multiple nonlinear regression was evaluated by comparing with a strain-dependent Arrhenius-type (SCA) constitutive equation.

Experimental details

The chemical composition (wt.%) of BFe10-1-2 alloy investigated in the present study is: Ni = 10.80, Mn = 2, Fe = 1.38, Cu = bal. And the original microstructure of as-received BFe10-1-2 alloy is shown in Figure 2.

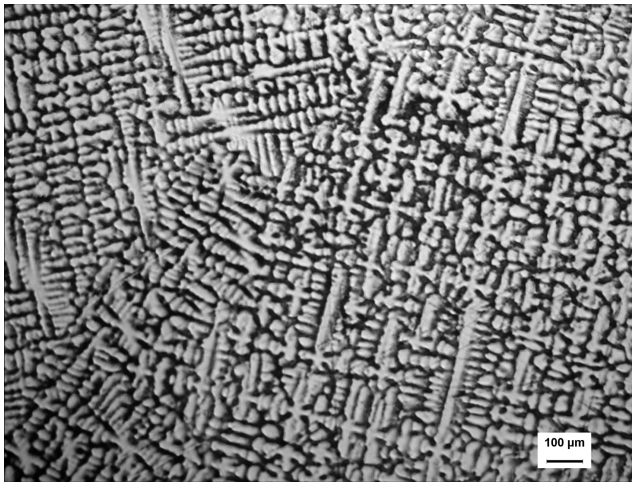

Figure 2: The microstructure of the original sample.

Cylindrical specimens were machined with a diameter of 10 mm and a height of 15 mm for compression tests. The flat ends of each specimen were recessed a depth of 0.1 mm groove to entrap the lubricant for the purpose of minimizing the friction. In order to obtain the heat balance, each specimen was heated to the deformation temperature at a rate of 10 K/s, and held for 3 min under the deformation conditions before compression tests. Then isothermal compression tests were carried out in the strain rate range of 0.001~10 s^{-1} and the temperature range of 1,023~1,273 K by a Gleeble-3800 simulator. After deformation, the specimens were cooled to room temperature in air, and the strain–stress curves were recorded automatically in isothermal compression.

Results and discussion

Flow stress

The flow stress curves obtained through hot compression tests are shown in Figure 3. It is clear that BFe10-1-2 alloy exhibits strain rate hardening and thermal softening. The flow stress increases with the increase of strain rate at a

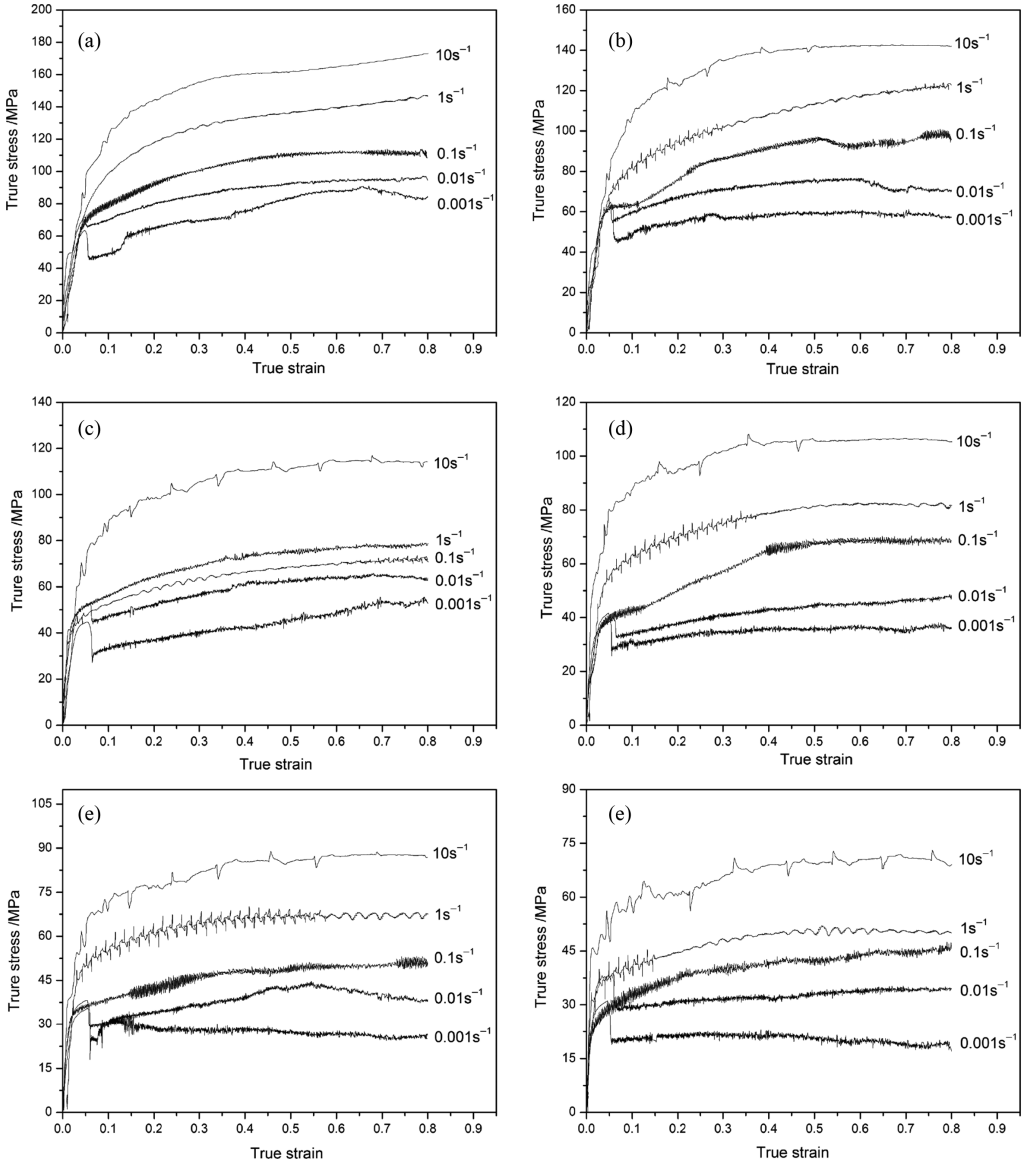

Figure 3: Flow curves of BFe10-1-2 alloy at various strain rates with temperatures of (a) 1,023 K, (b) 1,073 K (c) 1,123 K, (d) 1,173 K, (e) 1,223 K, (f) 1,273 K.

certain deformation temperature, and decreases with the increase of deformation temperature at a certain strain rate. Meanwhile, the flow stress increases quickly with the increase of strain in the initial stage due to the generation, multiplication and intersect of dislocation. Then, with the increase of deformation, a saturation flow stress appears and stays nearly constant, which indicates a dynamic recovery (DRV) characteristic of the metal material. In this stage, dislocation density increases and the interaction between dislocations becomes more significant. However, due to heat activation at high temperature, larger dislocation density will be annihilated and rearranged by the dislocation climbing, sliding and cross-slip, which leads to polygonization of dislocation and regularization of dislocation cell wall to further form subboundaries. When a balance between work hardening and DRV is reached, the flow stress remains near constant.

Modified double multivariate nonlinear regression

The constitutive equation of BFe10-1-2 alloy at high temperatures consists of flow stress and influence parameters. As shown in Figure 4, x_i ($i = 1, 2, 3$) are test factors (i. e., strain ε, strain rate $\dot{\varepsilon}$ and temperature T); y_j are material parameters ($j = 1, 2, 3, ...,9$), which indicate the single effect (solid lines) and the interactive effect (dashed lines) of x_i on the flow stress; ψ_j are the corresponding weights for y_j, which indicate the single effect (solid lines) and the interactive effect (dashed lines) of x_i on the amplitude of flow stress; f_j are analysis factors, reflecting the influence function of analysis factors on flow stress; σ represents the flow stress which is defined as the objective function and is a pan-function of test factors x_i and weight-function of analysis factors f_j, $\sigma = P(x_i) = W(f_j)$; and ω_j are converged weights, which represent the contributions of analysis factors f_j to the objective function σ.

Analysis factors f_j consist of two parts: material parameters y_i and corresponding weights ψ_j. Meanwhile, y_i and ψ_j are the functions of test factors x_i. Then, the objective function σ can be developed from the contribution function $W(f_j)$, in which the analysis factors f_j are obtained from the physical theory of plastic deformation as follows:

$$\sigma = N\varepsilon^n \tag{1}$$

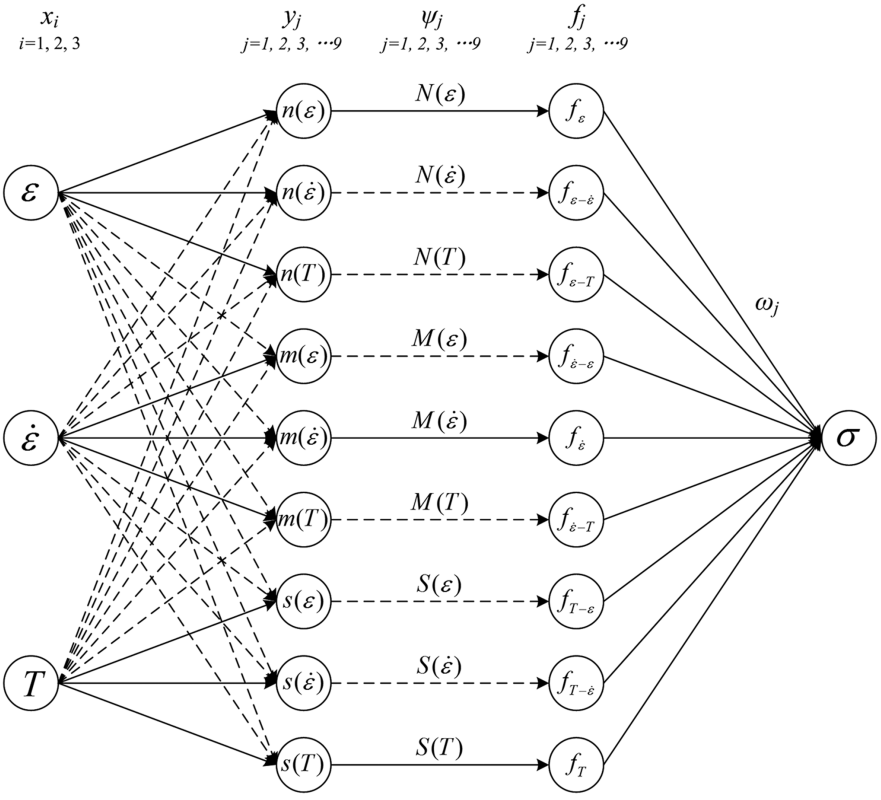

Figure 4: Relationship between flow stress and test factors as well as analysis factors.

$$\sigma = M\dot{\varepsilon}^{m} \tag{2}$$

$$\sigma = S\exp\left(\frac{mQ}{RT}\right) = S\exp\left(\frac{s}{T}\right) \tag{3}$$

where Q is the deformation activation energy ($J\cdot mol^{-1}$), R is the universal gas constant ($J\cdot mol^{-1}\cdot K^{-1}$), n, m and s are material parameters (y_i), and N, M and S are corresponding weights (ψ_j). Then taking natural logarithm of both sides of eqs (1)–(3) yields the following equations:

$$\ln\sigma = \ln N + n\ln\varepsilon \tag{4}$$

$$\ln\sigma = \ln M + m\ln\dot{\varepsilon} \tag{5}$$

$$\ln\sigma = \ln S + \frac{mQ}{RT} = \ln S + \frac{s}{T} \tag{6}$$

The contribution function $W(f_j)$ can be obtained by the nonlinear regression of experimental data, and the weights ω_j can be obtained by using the multivariate nonlinear regression. Therefore, the construction method for the constitutive equation can be called modified double multivariate nonlinear regression (i. e. nonlinear regression of contribution function $W(f_j)$ as well as objective function σ).

The mean flow stress values $\bar{\sigma}(x_i - x_i)$ are used to develop the constitution equation. For example, $\bar{\sigma}(\varepsilon - \dot{\varepsilon})$ is the mean value of flow stress at all temperatures, $\bar{\sigma}(\varepsilon - T)$ is the mean value of all strain rates, $\bar{\sigma}(\varepsilon)$ is the mean value of flow stress at all temperatures and strain rates, and $\sigma(\varepsilon, \dot{\varepsilon}, T)$ is the flow stress corresponding to the processing parameters. The specific process of establishing the constitution equation is given in Figure 5. K_ε, $K_{\dot{\varepsilon}}$, and K_T are the levels of strain, strain rate, and deformation temperature. In this research, the values of strain are selected in the range of 0.1~0.8 at an interval of 0.1, the strain rates are chosen as 0.001 s^{-1}, 0.01 s^{-1}, 0.1 s^{-1}, 1 s^{-1}

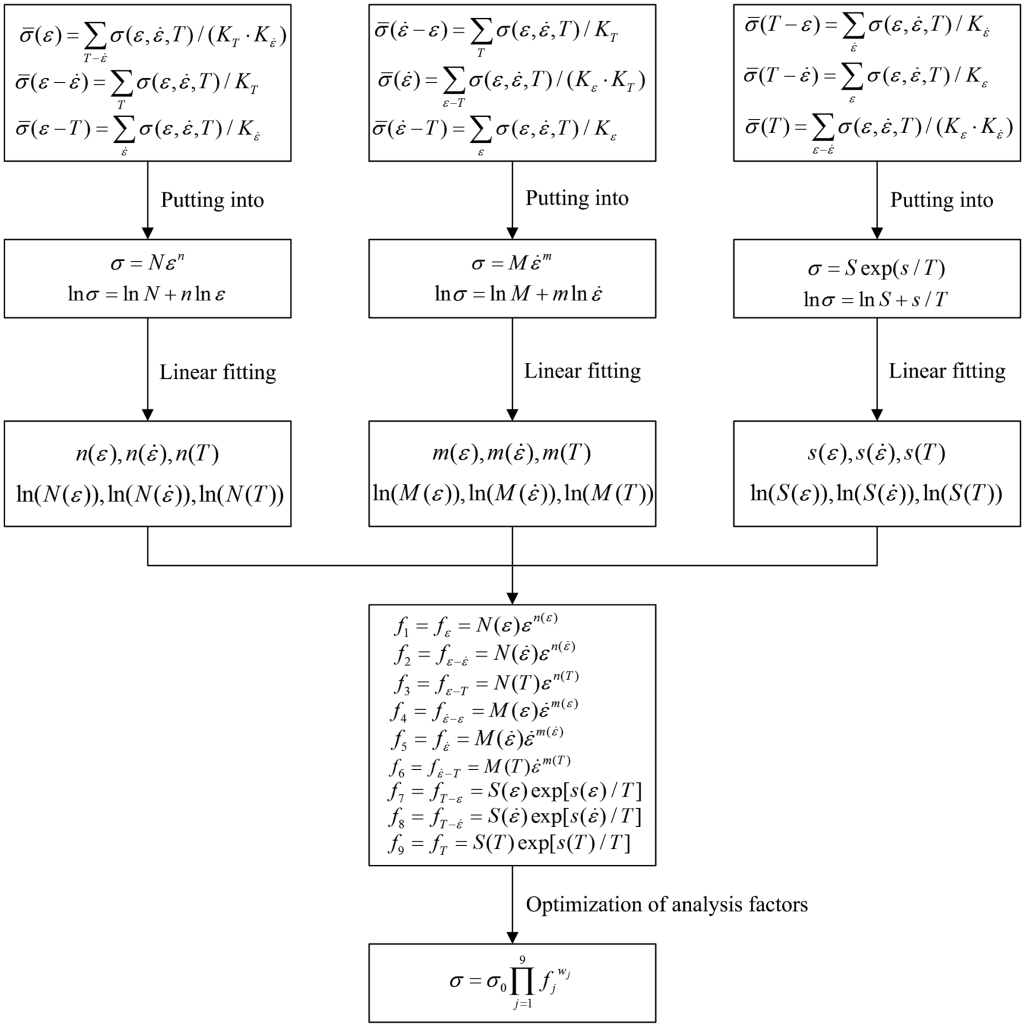

Figure 5: Diagram of determination for constitution equation based on modified double multiple nonlinear regression.

and 10 s^{-1}, and temperatures are selected as 1,023 K, 1,073 K, 1,123 K, 1,173 K, 1,223 K and 1,273 K. Accordingly, the values of K_ε, $K_{\dot\varepsilon}$, and K_T are 8, 5, and 6 respectively. Therefore, the whole analysis factors can be expressed as follows:

$$\begin{aligned} f_\varepsilon &= N(\varepsilon)\varepsilon^{n(\varepsilon)} \\ f_{\varepsilon-\dot\varepsilon} &= N(\dot\varepsilon)\varepsilon^{n(\dot\varepsilon)} \\ f_{\varepsilon-T} &= N(T)\varepsilon^{n(T)} \\ f_{\dot\varepsilon} &= M(\dot\varepsilon)\dot\varepsilon^{m(\dot\varepsilon)} \\ f_{\dot\varepsilon-\varepsilon} &= M(\varepsilon)\dot\varepsilon^{m(\varepsilon)} \\ f_{\dot\varepsilon-T} &= M(T)\dot\varepsilon^{m(T)} \\ f_{T-\varepsilon} &= S(\varepsilon)\exp[s(\varepsilon)/T] \\ f_{T-\dot\varepsilon} &= S(\dot\varepsilon)\exp[s(\dot\varepsilon)/T] \\ f_T &= S(T)\exp[s(T)/T] \end{aligned} \tag{7}$$

Determination of material parameters y_i

The mean stress $\bar\sigma(\varepsilon)$ at different levels can be obtained as follows:

$$\bar\sigma(\varepsilon) = \sum_{T-\dot\varepsilon} \sigma(\varepsilon, \dot\varepsilon, T)/(K_T \cdot K_{\dot\varepsilon}) \tag{8}$$

Figure 6 illustrates the relationship between $\ln(\bar\sigma(\varepsilon))$ and $\ln(\varepsilon)$. Then the values of $n(\varepsilon)$ and $\ln(N(\varepsilon))$ can be acquired as the slope and intercept in the plot of two adjacent points in Figure 6. Then, a cubic spline fit is employed to express the relationship between $n(\varepsilon)$ and strain (eq. (9)), and a fourth-order polynomial function is used to express the relationship between $\ln(N(\varepsilon))$ and strain (eq. (10)), as shown in Figure 7.

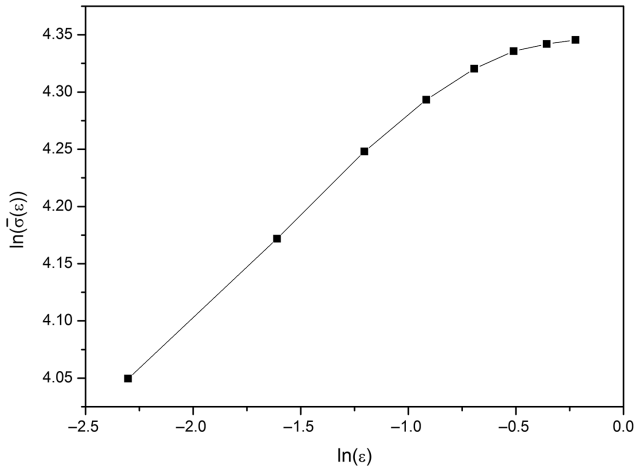

Figure 6: Relationship between $\ln(\bar\sigma(\varepsilon))$ and $\ln(\varepsilon)$.

$$n(\varepsilon) = 0.0998 + 0.89855\varepsilon - 2.72561\varepsilon^2 + 1.85993\varepsilon^3 \tag{9}$$

$$\begin{aligned} \ln(N(\varepsilon)) = 4.27838 + 2.23401\varepsilon - 8.37444\varepsilon^2 \\ + 11.32077\varepsilon^3 - 5.27472\varepsilon^4 \end{aligned} \tag{10}$$

The mean stress values of $\bar\sigma(\varepsilon - \dot\varepsilon)$ at different temperatures can be obtained as follows:

$$\bar\sigma(\varepsilon - \dot\varepsilon) = \sum_T \sigma(\varepsilon, \dot\varepsilon, T)/K_T \tag{11}$$

Therefore, the values of $n(\dot\varepsilon)$ and $\ln(N(\dot\varepsilon))$ can be derived from the slopes and intercepts of the lines of $\ln(\bar\sigma(\varepsilon - \dot\varepsilon)) - \ln(\varepsilon)$, as shown in Figure 8. The relationships of $n(\dot\varepsilon)$-$\ln(\dot\varepsilon)$ and $\ln(N(\dot\varepsilon))$-$\ln(\dot\varepsilon)$ are illustrated in Figure 9. A cubic spline fit and a linear fit can be found to represent $n(\dot\varepsilon)$ and $\ln(N(\dot\varepsilon))$ respectively:

$$\begin{aligned} n(\dot\varepsilon) = 0.16675 - 0.00703\ln(\dot\varepsilon) - 0.00422(\ln(\dot\varepsilon))^2 \\ - 0.000372(\ln(\dot\varepsilon))^3 \end{aligned} \tag{12}$$

$$\ln(N(\dot\varepsilon)) = 4.58142 + 0.09747\ln(\dot\varepsilon) \tag{13}$$

Similarly, the values of $n(T)$ and $\ln(N(T))$ are acquired from the slopes and intercepts of the lines of $\ln(\bar\sigma(\varepsilon - T)) - 1/T$. The relationship of $n(T)$-$T/100$ and $\ln(N(T))$-$T/100$ is illustrated in Figure 10. A fourth spline fit and a linear fit are used to represent $n(T)$ and $\ln(N(T))$ respectively:

$$\begin{aligned} n(T) = 784.40233 - 275.2801(T/100) + 36.15935(T/100)^2 \\ - 2.10636(T/100)^3 + 0.04591(T/100)^4 \end{aligned} \tag{14}$$

$$\ln(N(T)) = 9.09012 - 0.41336(T/100) \tag{15}$$

Similarly, $m(x_i)$, $s(x_i)$, $\ln(M(x_i))$ and $\ln(S(x_i))$ can also be obtained in the same method. It should be noted that the relationships of $\ln(\sigma(\dot\varepsilon)) - \ln(\dot\varepsilon)$ and $\ln(\sigma(T)) - 1000/T$ exhibit obvious linear relationship. Therefore, the values of $m(\dot\varepsilon)$ and $s(T)$ can be obtained from the slops of Figure 11(a) and (b) as 0.09768 as well as 4,964.82, and the values of $\ln(M(\dot\varepsilon))$ and $\ln(S(T))$ can be acquired from the interrupts as 4.44243 and −0.13432.

Subsequently, $m(x_i)$, $s(x_i)$, $\ln(M(x_i))$ and $\ln(S(x_i))$ varying with strain, strain rate and temperature are given in Figures 12 and 13, respectively.

Furthermore, the equations of $m(\varepsilon)$, $m(T)$, $s(\varepsilon)$, $s(\dot\varepsilon)$, $\ln(M(\varepsilon))$, $\ln(M(T))$, $\ln(S(\varepsilon))$ and $\ln(S(\dot\varepsilon))$ can be obtained as follows:

$$\begin{aligned} m(\varepsilon) = 0.13435 - 0.783681\varepsilon + 5.79876\varepsilon^2 - 19.70598\varepsilon^3 \\ + 33.79071\varepsilon^4 - 28.60096\varepsilon^5 + 9.54167\varepsilon^6 \end{aligned} \tag{16}$$

$$\ln(M(\varepsilon)) = 4.05261 + 1.98782\varepsilon - 2.96002\varepsilon^2 + 1.51452\varepsilon^3 \tag{17}$$

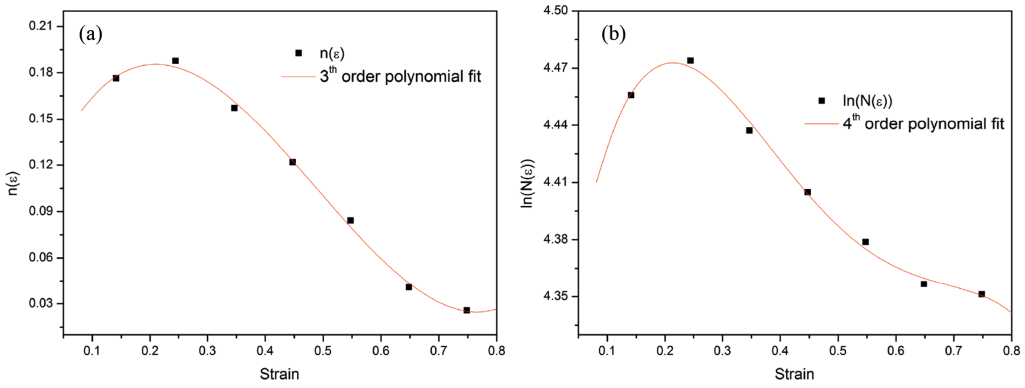

Figure 7: Relationship between (a) $n(\varepsilon)$-ε; and (b) $\ln(N(\varepsilon))$-ε.

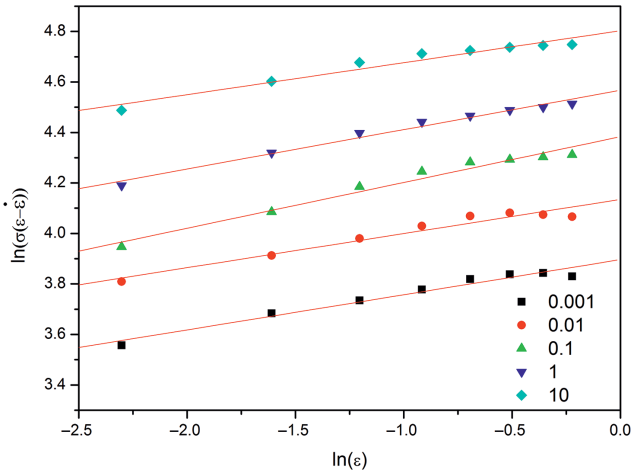

Figure 8: Relationship between $\ln(\bar{\sigma}(\varepsilon-\dot{\varepsilon}))$ and $\ln(\varepsilon)$.

$$m(T) = 12.39424 - 32.76451(T/1000) + 28.85334(T/1000)^2 - 8.3963(T/1000)^3 \quad (18)$$

$$\ln(M(T)) = 8.50888 - 3.58457(T/1000) \quad (19)$$

$$s(\varepsilon) = 3.65885 + 7.55309\varepsilon - 13.78552\varepsilon^2 + 8.62447\varepsilon^3 \quad (20)$$

$$\ln(S(\varepsilon)) = 1.15185 - 12.17409\varepsilon + 41.45719\varepsilon^2 - 59.07629\varepsilon^3 + 29.26326\varepsilon^4 \quad (21)$$

$$s(\dot{\varepsilon}) = 4.79203 - 0.09238\ln(\dot{\varepsilon}) - 0.0361(\ln(\dot{\varepsilon}))^2 - 0.00909(\ln(\dot{\varepsilon}))^3 \quad (22)$$

$$\ln(S(\dot{\varepsilon})) = 0.1708 + 0.1815\ln(\dot{\varepsilon}) + 0.03764(\ln(\dot{\varepsilon}))^2 + 0.00884(\ln(\dot{\varepsilon}))^3 \quad (23)$$

Determination of major analysis factors

Then, the contribution functions of the independent factors (f_ε, $f_{\dot{\varepsilon}}$ and f_T) and interactive factors ($f_{\varepsilon-\dot{\varepsilon}}$, $f_{\varepsilon-T}$, $f_{\dot{\varepsilon}-\varepsilon}$, $f_{\dot{\varepsilon}-T}$, $f_{T-\varepsilon}$ and $f_{T-\dot{\varepsilon}}$) can be easily obtained. As discussed above, analysis factors f_j are composed of material parameters y_i and corresponding weights ψ_j. It should be noted that some factors may have significant influence

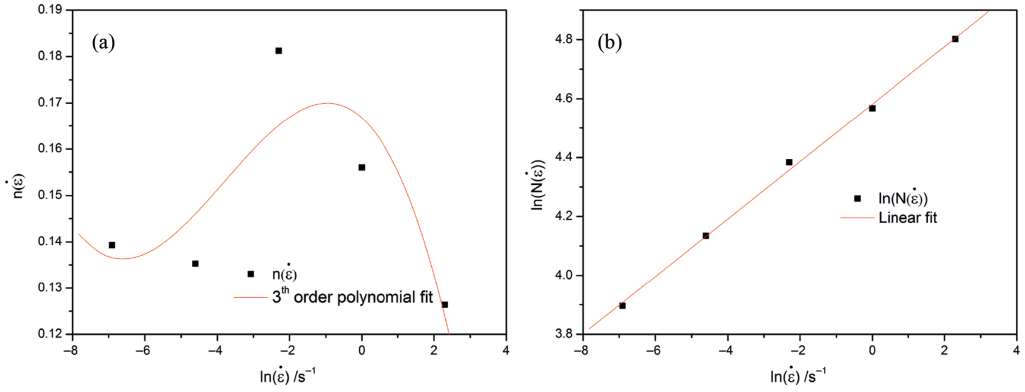

Figure 9: Relationship between (a) $n(\dot{\varepsilon})$ and $\ln(\dot{\varepsilon})$; (b) $\ln(N(\dot{\varepsilon}))$-$\ln(\dot{\varepsilon})$.

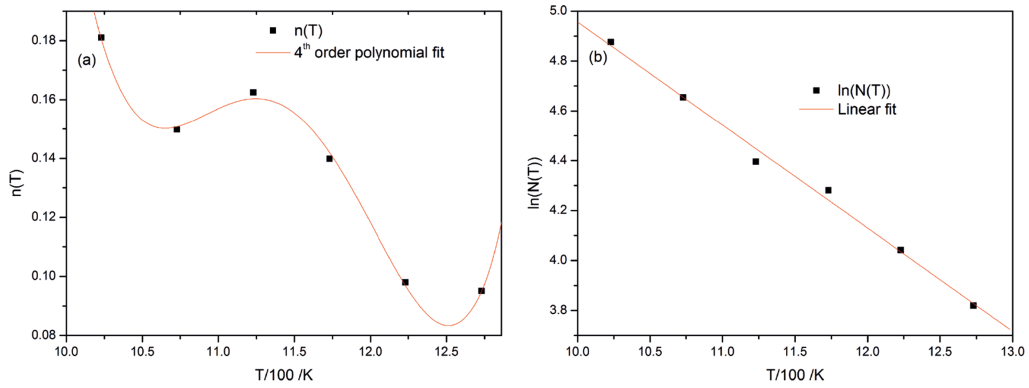

Figure 10: Relationship between (a) $n(T)$ and $T/100$; (b) $\ln(N(T))$ and $T/100$.

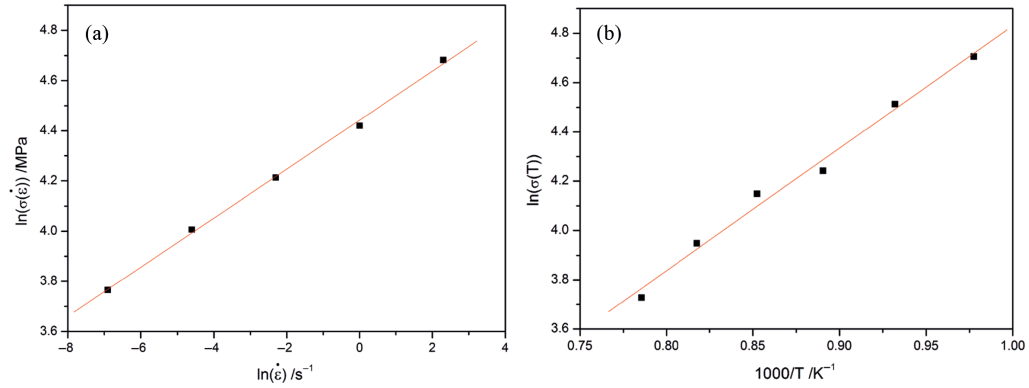

Figure 11: Relationship between (a) $\ln(\sigma(\dot{\varepsilon}))$ and $\ln(\dot{\varepsilon})$; (b) $\ln(\sigma(T))$ and $1,000/T$.

on the flow stress while the others may have few contributions. Therefore, it is essential to find out the primary analysis factors. The mean value (*MV*), standard deviation (*SD*) and coefficient of variance (*CV*) are employed to analyze the analysis factors. As is well known, *MV* can represent the overall level, *SD* can reflect the discrete degree of a data set, and *CV* can better reflect the discrete degree of data ($CV = MV/SD$). SD can be expressed as follows:

$$SD = \sqrt{\frac{\sum_{i=1}^{V} (f_i - \bar{f})^2}{V-1}} \tag{24}$$

where V is the sample number. The order of *CV* about analysis factors is given in Table 1. It can be seen from the table that the value of *CV* for f_ε is less than 10 % (9.68 %), which indicates that the strain has little influence on the flow stress, and can be ignored in constitutive equation. However, the values of other *CV* are much higher than 10 %, which indicate the influence of these factors on flow stress is significant. Meanwhile, the interactive effect of strain rate and temperature has greater influence than other factors. Therefore, $f_{T-\dot{\varepsilon}}$, $f_{\dot{\varepsilon}-T}$, $f_{\varepsilon-T}$, $f_{T-\varepsilon}$, $f_{\dot{\varepsilon}}$, $f_{\varepsilon-\dot{\varepsilon}}$, f_T, and $f_{\dot{\varepsilon}-\varepsilon}$ are selected as the major analysis factors.

Determination of the converged weights

The constitutive equation of material during plastic deformation during high temperature can be expressed as:

$$\sigma = \sigma(\varepsilon, \dot{\varepsilon}, T) \tag{25}$$

On the basis of orthogonal test and variance analysis, a comprehensive constitutive equation incorporating the effects of strain, strain rate and temperature is derived as follows [10]:

$$\sigma = \sigma_0 f_\varepsilon f_{\dot{\varepsilon}} f_T \tag{26}$$

where σ_0 is the initial yield stress, and f_ε, $f_{\dot{\varepsilon}}$, and f_T are the influence functions of strain, strain rate and temperature, respectively. The interaction among the single

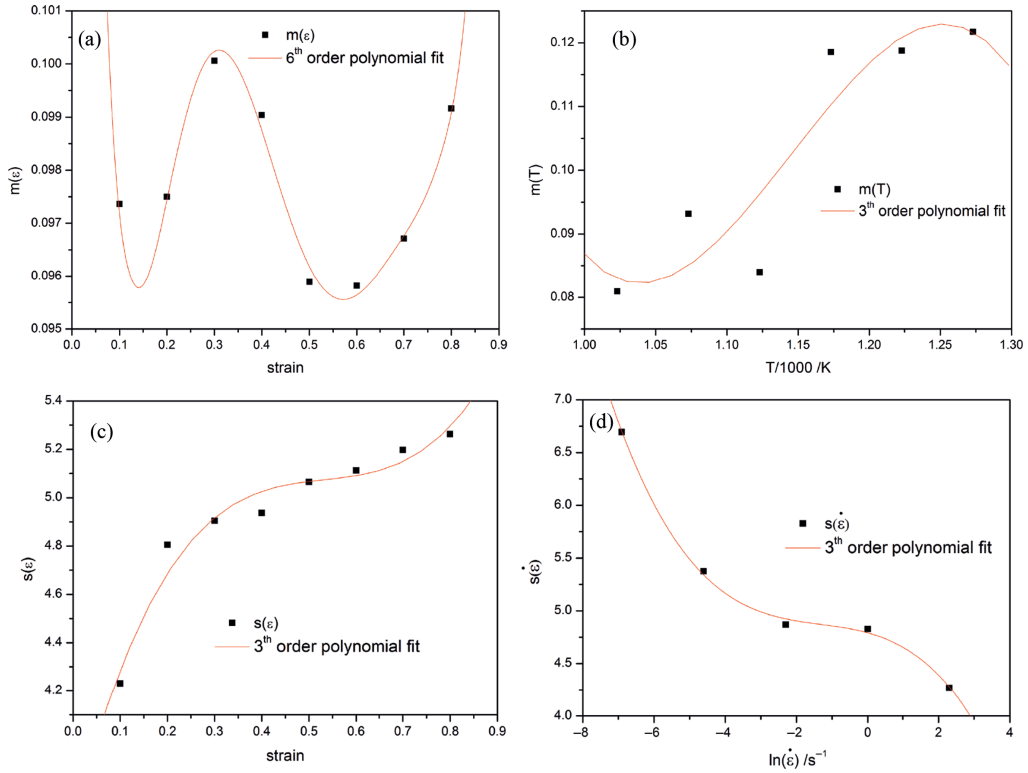

Figure 12: *m*, *s* changing with strain, strain rate and temperature: (a) $m(\varepsilon)$; (b) $m(T)$; (c) $s(\varepsilon)$; (d) $s(\dot{\varepsilon})$.

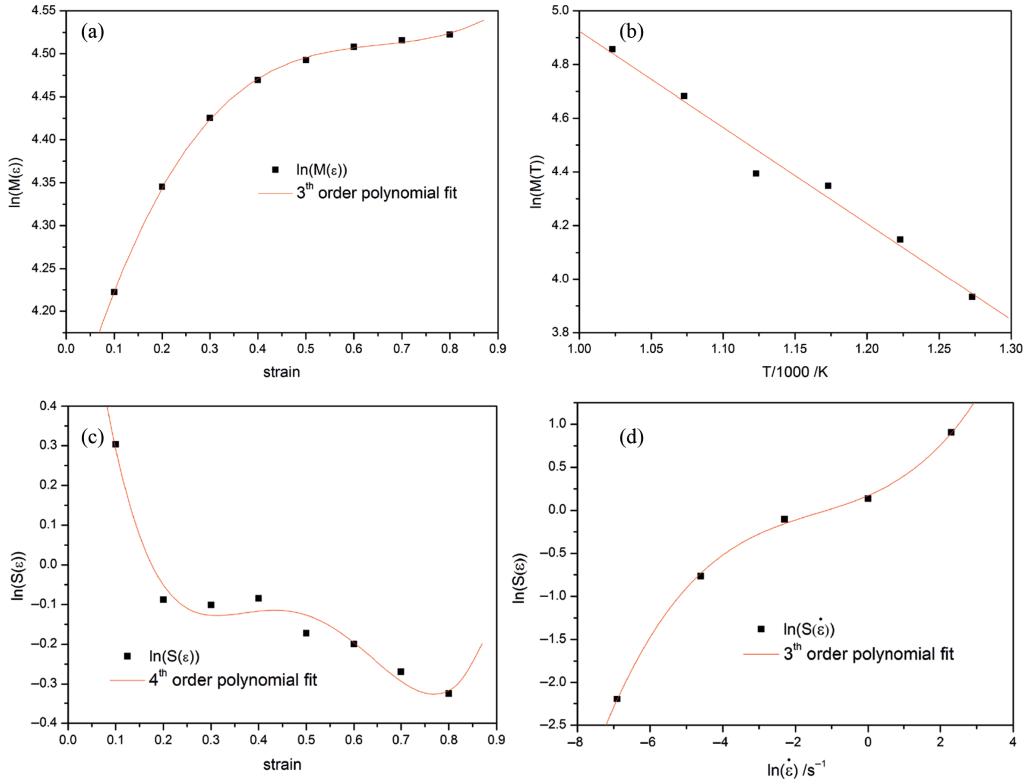

Figure 13: ln(*M*), ln(*S*) changing with strain, strain rate and temperature: (a) $\ln(M(\varepsilon))$; (b) $\ln(M(T))$; (c) $\ln(S(\varepsilon))$; (d) $\ln(S(\dot{\varepsilon}))$.

Table 1: The order of CV about analysis factors.

	Analysis factor	MV	SD	*CV* (%)
1	$f_{T-\dot{\varepsilon}}$	71.341	33.4938	46.95
2	$f_{\dot{\varepsilon}-T}$	71.234	32.8244	46.08
3	$f_{\varepsilon-T}$	67.889	24.9727	36.78
4	$f_{T-\varepsilon}$	71.4417	25.2493	35.34
5	$f_{\dot{\varepsilon}}$	71.3472	25.0487	35.11
6	$f_{\varepsilon-\dot{\varepsilon}}$	71.6435	23.6573	33.02
7	f_T	71.3718	23.5453	32.99
8	$f_{\dot{\varepsilon}-\varepsilon}$	71.3414	23.7498	32.38
9	f_{ε}	71.4789	6.9193	9.68

factors has been ignored for the purpose of simplifying the calculation process. However, it can be seen from Table 1 that the interaction among the single factors has significant influence on the flow stress, and the accuracy of constitutive equation may be reduced because of ignoring of some primary interaction. Therefore, eq. (26) can be modified as follows:

$$\sigma = \sigma(\varepsilon, \dot{\varepsilon}, T) = \sigma_0 f_{T-\dot{\varepsilon}} f_{\dot{\varepsilon}-T} f_{\varepsilon-T} f_{T-\varepsilon} f_{\dot{\varepsilon}} f_{\varepsilon-\dot{\varepsilon}} f_T f_{\dot{\varepsilon}-\varepsilon} \tag{27}$$

By considering the converged weights ω_j, eq. (27) can be modified as follows:

$$\sigma = \sigma(\varepsilon, \dot{\varepsilon}, T) = \sigma_0 f_{T-\dot{\varepsilon}}{}^{\omega_1} f_{\dot{\varepsilon}-T}{}^{\omega_2} f_{\varepsilon-T}{}^{\omega_3} f_{T-\varepsilon}{}^{\omega_4} f_{\dot{\varepsilon}}{}^{\omega_5} f_{\varepsilon-\dot{\varepsilon}}{}^{\omega_6} f_T{}^{\omega_7} f_{\dot{\varepsilon}-\varepsilon}{}^{\omega_8} \tag{28}$$

Taking the natural logarithm of both sides of eq. (28) yields:

$$\begin{aligned} \ln\sigma = {} & \ln\sigma_0 + \omega_1 \ln f_{T-\dot{\varepsilon}} + \omega_2 \ln f_{\dot{\varepsilon}-T} + \omega_3 \ln f_{\varepsilon-T} + \omega_4 \ln f_{T-\varepsilon} \\ & + \omega_5 \ln f_{\dot{\varepsilon}} + \omega_6 \ln f_{\varepsilon-\dot{\varepsilon}} + \omega_7 \ln f_T + \omega_8 \ln f_{\dot{\varepsilon}-\varepsilon} \end{aligned} \tag{29}$$

As is well known, multivariate regression (MR) analysis is a highly flexible system for examining the relationship between a collection of the independent variable and dependent variable. Therefore, the present study explores least square regression with independent variable $\ln f_j$ and dependent variable $\ln\sigma$. Through the MR test via SPSS software, the correction coefficient σ_0 and the converged weights ω_1, ω_2, ω_3, ω_4, ω_5, ω_6, ω_7 and ω_8 are obtained, as shown in Table 2.

Table 2: The values of σ_0 and ω_j obtained by multivariate linear regression.

σ_0	ω_1	ω_2	ω_3	ω_4	ω_5	ω_6	ω_7	ω_8
1.19	0.943	0.061	0.569	0.183	−0.011	−0.115	−0.787	0.123

Verification of the developed constitutive equations

In order to verify the developed constitutive equation based on modified double multiple nonlinear regression for BFe10-1-2 alloy, a comparison between the experimental and predicted flow stress data is carried out in Figure 14. As can be seen from Figure 14, the predicted flow stress data can track the experimental data of BFe10-1-2 alloy, and there is a good agreement between the experimental and predicted values under most deformation conditions. Only at one processing condition (i. e. at 1,123 K in 1 s^{-1}), an obvious variation between experimental and calculated flow stress data can be observed, as shown in Figure 14(c).

The predictability of the developed constitutive equation is quantified in terms of standard statistical parameters such as correlation coefficient (R) and average absolute relative error (*AARE*). These are expressed as follows [12]:

$$R = \frac{\sum_{i=1}^{C}(E_i - \bar{E})(P_i - \bar{P})}{\sqrt{\sum_{i=1}^{C}(E_i - \bar{E})^2 \sum_{i=1}^{C}(P_i - \bar{P})^2}} \tag{30}$$

$$AARE(\%) = \frac{1}{C}\sum_{i=1}^{C}\left|\frac{E_i - P_i}{E_i}\right| \times 100 \tag{31}$$

where E is the experimental flow stress and P is the predicted flow stress obtained from the developed constitutive equation. $\bar{E}$ and $\bar{P}$ are the mean values of E and P respectively. C is the total number of data used in this study. R is a commonly employed statistical parameter and provides information on the strength of the linear relationship between the experimental and predicted data. *AARE* is calculated through a term by term comparison of the relative error and is an unbiased statistical parameter for determining the predictability of the equation. The correlation between experimental flow stresses and predicted data is shown in Figure 15. It can be seen from figure that most of the data points are located close to the fitting lines, and the values of R and *AARE* are found to be 0.9913 and 5.248 % respectively.

Meanwhile, the performance of the developed constitutive equation is further investigated by statistical analysis of the relative error. The predictions are compared with the corresponding experimental data, and subsequently the relative errors are expressed as [13]:

$$\text{relative error} = \left(\frac{E_i - P_i}{E_i}\right) \times 100\% \tag{32}$$

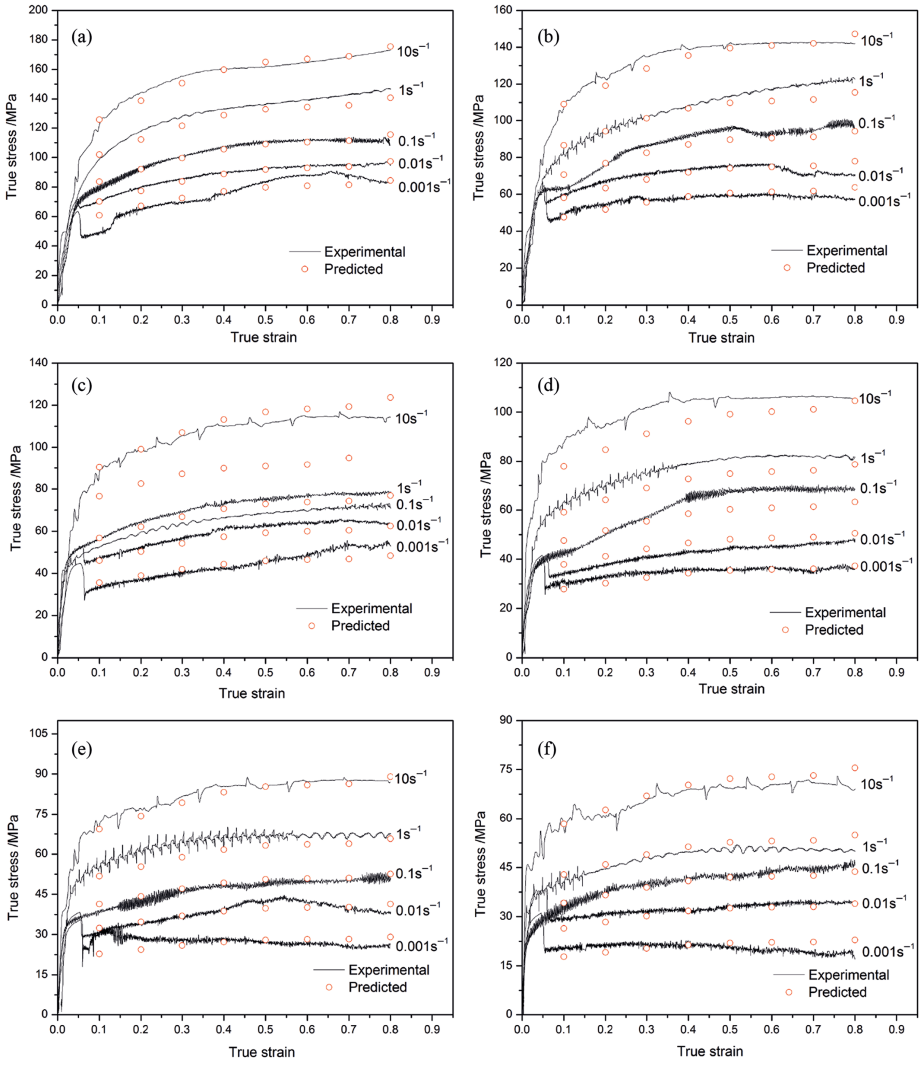

Figure 14: Comparison of the experimental and predicted values by the Arrhenius-type constitutive equation at the temperature of (a) 1,023 K, (b) 1,073 K, (c) 1,123 K, (d) 1,173 K, (e) 1,223 K, (f) 1,273 K.

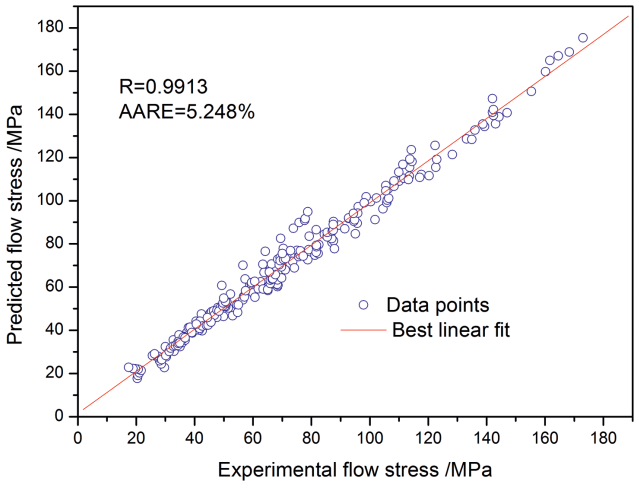

Figure 15: Correlation between the experimental and predicted flow stress data.

The results of relative error are represented graphically as a typical number versus error plot, as illustrated in Figure 16. As can be seen from Figure 16, the relative errors exhibit Gaussian distribution, and vary from –31.53 % to 23.34 %. The mean value of the relative errors is only –0.129. Therefore, the modified double multiple nonlinear regression constitutive equation gives an accurate and precise estimate of the flow stress of BFe10-1-2 alloy.

Comparison with SCA constitutive model

Nowadays, Arrhenius-type constitutive model is widely used to describe the high temperature flow behavior of metals, especially at elevated temperatures. This model exhibits higher accuracy than the JC, modified JC and

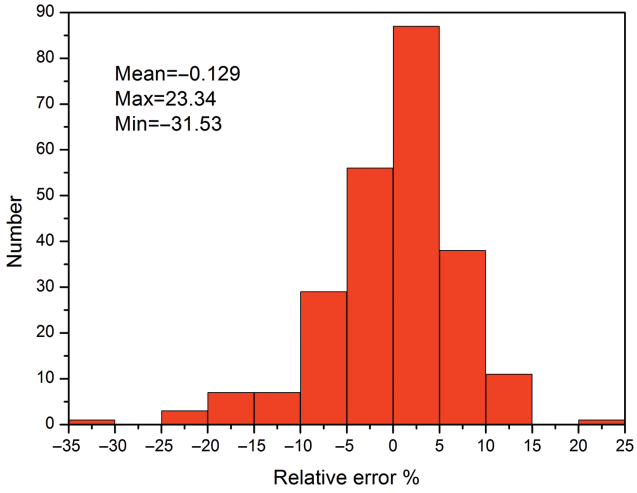

Figure 16: Statistical analysis of the relative error.

modified ZA models, and this has been proved in 9Cr-1Mo steel [14], 28CrMnMoV steel [15], Mg-6Al-1Zn alloy [16], and 7050 aluminum alloy [17]. The Arrhenius-type constitutive equation can be expressed in the following form:

$$\sigma = \frac{1}{\alpha}\ln\left\{\left(\frac{Z}{A}\right)^{1/n} + \left[\left(\frac{Z}{A}\right)^{2/n} + 1\right]^{1/2}\right\} \tag{33}$$

where A, α and n are the materials constants, and Z is Zener-Hollomon parameter and expressed as:

$$Z = \dot{\varepsilon}\exp\left(\frac{Q}{RT}\right) \tag{34}$$

The influence of strain on the Arrhenius-type constitutive equation is incorporated by assuming that the material constants (i. e. α, n, Q and lnA) are polynomial function of strains. In the authors' previous study, a third- and a sixth-order polynomial is founded to represent the influence of the strain on α as well as other material constants (i. e. n, Q and lnA) with a good correlation and generalization, as shown in eq. (35) and Table 3 [18].

$$\begin{aligned}
\alpha &= C_0 + C_1\varepsilon + C_2\varepsilon^2 + C_3\varepsilon^3 \\
n &= D_0 + D_1\varepsilon + D_2\varepsilon^2 + D_3\varepsilon^3 + D_4\varepsilon^4 + D_5\varepsilon^5 + D_6\varepsilon^6 \\
Q &= E_0 + E_1\varepsilon + E_2\varepsilon^2 + E_3\varepsilon^3 + E_4\varepsilon^4 + E_5\varepsilon^5 + E_6\varepsilon^6 \\
\ln A &= F_0 + F_1\varepsilon + F_2\varepsilon^2 + F_3\varepsilon^3 + F_4\varepsilon^4 + F_5\varepsilon^5 + F_6\varepsilon^6
\end{aligned} \tag{35}$$

Figure 17 illustrates the correlation between the experimental and predicted flow stress data from the SCA constitutive equation. The value of R for SCA constitutive model is 0.988, which is lower than that of the modified double multiple nonlinear regression constitutive equation (0.9913), while the value $AARE$ (5.663 %) is higher than that of the modified multiple nonlinear regression constitutive equation (5.248 %). Meanwhile, the mean value of the relative errors for the SCA constitutive equation is −0.956 (shown in Figure 18), whereas the value is −0.129 for the modified multiple nonlinear regression constitutive equation. Therefore, the developed constitutive equation based on modified multiple nonlinear regression shows a better correlation between the predicted results and experimental data than strain compensated Arrhenius-type model.

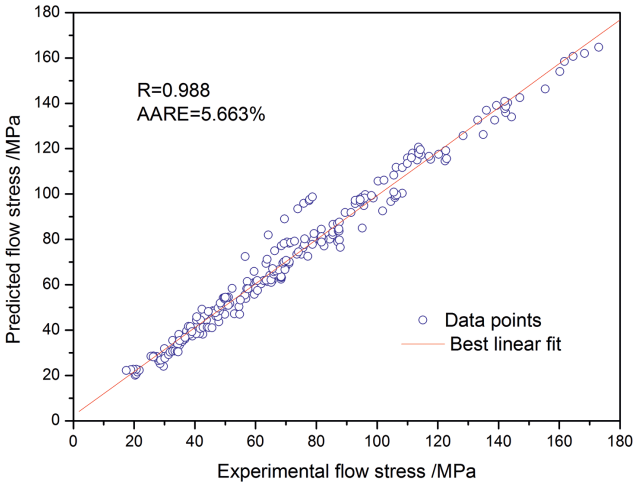

Figure 17: Correlation between the experimental and predicted flow stress data from SCA constitutive equation.

Table 3: Coefficients of the polynomial for α, n, Q, and lnA.

A	*N*	*Q*	*lnA*
$C_0 = 0.02024$	$D_0 = 6.20894$	$E_0 = 21.10058$	$F_0 = -0.67266$
$C_1 = -0.02953$	$D_1 = 31.99133$	$E_1 = 6555.486$	$F_1 = 684.9015$
$C_2 = 0.04911$	$D_2 = -259.465$	$E_2 = -42377.4$	$F_2 = -4431.61$
$C_3 = -0.02689$	$D_3 = 916.6475$	$E_3 = 134955.2$	$F_3 = 14120.23$
	$D_4 = -1620.57$	$E_4 = -224483$	$F_4 = -23519.7$
	$D_5 = 1414.3363$	$E_5 = 188005.64$	$F_5 = 19732.991$
	$D_6 = -487.054$	$E_6 = -62743.2$	$F_6 = -6596.96$

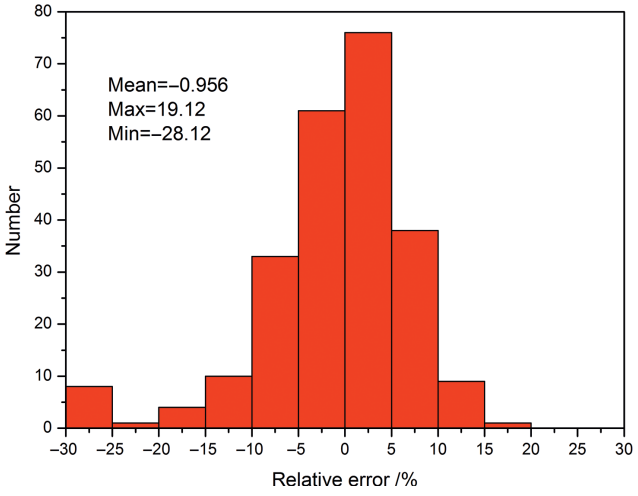

Figure 18: Statistical analysis of the relative error for SCA constitutive equation.

Conclusions

A constitutive equation based on modified double multiple nonlinear regression of BFe10-1-2 alloy was developed by performing high temperature compression tests in a wide range of temperatures (1,023–1,273 K) and strain rates (0.001–10 s^{-1}). Based on this study, following are the conclusions:

(1) A modified double multiple nonlinear regression constitutive equation was proposed to predict the high temperature flow behavior of BFe10-1-2 alloy by taking into accounts the independent factors and coupled effects of processing parameters.

(2) The predictability of the developed constitutive equation was quantified in terms of *R*, *AARE*, and relative errors. The results show that the modified double multiple nonlinear regression constitutive equation gives an accurate and precise estimate of the flow stress of BFe10-1-2 alloy.

(3) The predictability of modified double multiple nonlinear regression constitutive equation is comparable to that of SCA constitutive equation. The result showed that modified double multiple nonlinear regression constitutive equation shows a relatively higher accuracy than SCA model.

Acknowledgments: The authors gratefully acknowledge the financial support received from Planned Scientific Research Project of Education Department of Shaanxi Provincial Government (15JS056), Pre-research Foundation of Jinchuan company-Xi'an University of Architecture and Technology (YY1501), Project of International Cooperation and Exchange of Shaanxi Provincial (2016KW-054).

References

[1] S.B. Lalvani, J.C. Kang and N.V. Mandich, Corros. Sci., 40 (1998) 69–89.
[2] S. Martinez and M. Metikos-Hukovic, J.Appl. Electrochem., 36 (2006) 1311–1315.
[3] C. Zhang, L.W. Zhang, W.F. Shen, M.F. Li and S.D. Gu, J. Mater Eng. Peform., 24 (2015) 149–157.
[4] M.Z. Hussain, F.G. Li, J. Wang, Z.W. Yuan, P. Li and T. Wu, J. Mater. Eng. Peform., 24 (2015) 2744–2756.
[5] Y.C. Lin and X.M. Chen, Mater. des., 32 (2011) 1733–1759.
[6] W.S. Lee and C.Y. Liu, Metall. Mater. Trans. A, 36 (2005) 3175–3185.
[7] T. Zhang, Y.R. Tao and X.Y. Wang, Trans. Nonferrous Met. Soc. China, 24 (2014) 1337–1345.
[8] M.Q. Li, H.S. Pan, Y.Y. Lin and J. Luo, Mater. Process. Technol., 183 (2007) 71–76.
[9] J.C. Shao, B.L. Xiao, Q.Z. Wang, Z.Y. Ma, Y. Liu and K. Yang, Mater. Sci. Eng. A, 527 (2010) 7865–7872.
[10] M.L. Xiao, F.G. Li, W. Zhao and G.L. Yang, Mater. Des., 35 (2012) 184–193.
[11] Z.W. Yuan, F.G. Li, H.J. Qiao, M.L. Xiao, J. Cai and J. Li, Mater. Sci. Eng. A, 578 (2013) 260–270.
[12] S. Mandal, P.V. Sivaprasad, S. Venugopal and K.P.N. Murthy Appl, . Soft Comput J. ., 9 (2009) 237–244.
[13] H.Y. Li, X.F. Wang, D.D. Wei, J.D. Hu and Y.H. Li, Mater. Sci. Eng. A, 536 (2012) 216–222.
[14] D. Samantaray, S. Mandal and A.K. Bhaduri, Comput. Mater. Sci., 47 (2009) 568–576.
[15] H.Y. Li, Y.H. Li, X.F. Wang, J.J. Liu and Y. Wu, Mater. Des., 49 (2013) 493–501.
[16] A. Abbasi-Bani, A. Zarei-Hanzaki, M.H. Pishbin and N. Haghdadi, Mech. Mater., 71 (2014) 52–61.
[17] J. Li, F.G. Li, J. Cai, R.T. Wang, Z.W. Yuan and G.L. Ji, Comput. Mater. Sci., 71 (2013) 56–65.
[18] J. Cai, K.S. Wang, C.P. Miao, W.B. Li, W. Wang and J. Yang, Mater. Des., 65 (2015) 272–279.